Bulletin of Earth Sciences of Thailand

Seismicity rate change along the strike-slip fault system at the Thailand-Myanmar border: Implications for upcoming earthquakes

Santi Pailoplee[1,*], Narit Panwoon[1] and Parisa Nimnate[2]

[1]*Morphology of Earth Surface and Advanced Geohazards in Southeast Asia Research Unit (MESA RU), Department of Geology, Faculty of Science, Chulalongkorn University, Bangkok 10330, Thailand*
[2]*Division of Geosciences, Mahidol University, Kanchanaburi Campus, Saiyok,Kanchanaburi, 71150, Thailand*
* Corresponding author e-mail: Pailoplee.S@gmail.com

Received: 12 Jul 2021
Revised: 7 Feb 2022
Accepted: 14 Feb 2022

Abstract

In this study, both the temporal and spatial distributions of the seismicity rate changes were examined along the strike-slip fault system (SSFS) at the Thailand-Myanmar border. Based mainly on the completeness seismicity data, the relationships between the rate change anomalies and the proceeding earthquakes were checked empirically. Utilizing the obtained optimal condition of N = 25 events and Tw = 2 y, the results revealed that the lower the seismicity rate, the higher the probability of a subsequent earthquake occurrence. Hence, both spatial and temporal distributions of the rate changes were evaluated from the present-day seismicity data for 2005–2016. The maximum obtained Z value (7.3) was found in (i) 2006.43–2007.12 and 2012.64–2013.07 at northwestern Naypyidaw (96.50°E, 20.39°N) and (ii) in 2012.49 at the northeastern part of the SSFS (97.75°E, 21.89°N). This agrees well with those areas proposed previously by analysis of the frequency-magnitude distribution b-value. Therefore, effective mitigation plans should be contributed urgently, for Naypyidaw, the new capital city of Myanmar.

Keywords: seismicity rate, Z value, seismic quiescence, strike-slip fault system, Thailand, Myanmar

1. INTRODUCTION

Seismotectonically, the strike-slip fault system (SSFS), delineating along the Thailand-Myanmar border (Figure 1; Pailoplee et al., 2009), is defined as an intraplate regime according to the present-day seismicity of the Indian-Eurasian collision. Within this fault system, a lot of seismogenic fault zones have been proposed, including the Mae Hongsorn-Tak, Moei-Tongyi, Pan Luang, Pa Pun, Shan, Sri Sawath (SSFZ), Tavoy and Three Pagoda (TPFZ) fault zones (Nutalaya et al., 1985; Pailoplee et al., 2009). With respect to earthquake hazards, the SSFS is important due to its strike in the NW-SE direction and that the southern and northern parts are really close to Bangkok and Naypyidaw, the capital cities of Thailand and Myanmar, respectively. Furthermore, there are seven hydropower dams that are currently in operation in western Thailand and one that is planned for construction in eastern Myanmar (Figure 1).

Geological evidence has revealed that the SSFS, in particular for the TPFZ, has been moving in at least three stages with a different sense of movement (Rhodes et al., 2004). The rates of fault slips have been estimated variously at 0.22–2.87 mm/y (e.g., Nuttee et al., 2005; Department of Mineral Resources, 2007; Charusiri et al., 2011). In addition, Pailoplee and Charusiri (2016) reported that at least 10 paleoearthquakes have been posed in both the TPFZ and the SSFZ.

For the present-day seismic activities, Pailoplee (2014) determined the earthquake activities spatially along the SSFS using the frequency-magnitude distribution (FMD) model of earthquakes (Gutenberg and Richter, 1944). Both the possible maximum earthquake in a specific time span (10–50 y) and the recurrence interval of a given earthquake magnitude (4.0–7.0 M_w) were estimated. For instance, the possible maximum earthquake in the next 50 y was around 5.6 M_w along the northern segment, which is equal to that posed in the northern SSFZ in 1978, while the shortest recurrence intervals were located around the northern part of the SSFS and increased gradually towards the southern parts. In addition, according to the spatial distribution of the

FMD b-value, Pailoplee (2016) proposed five areas exhibiting low b-values as prospective areas of forthcoming earthquakes along the SSFS. As a result, most of the fault zones in this region were defined as hazardous seismic sources, and in particular for the northern part of the SSFS.

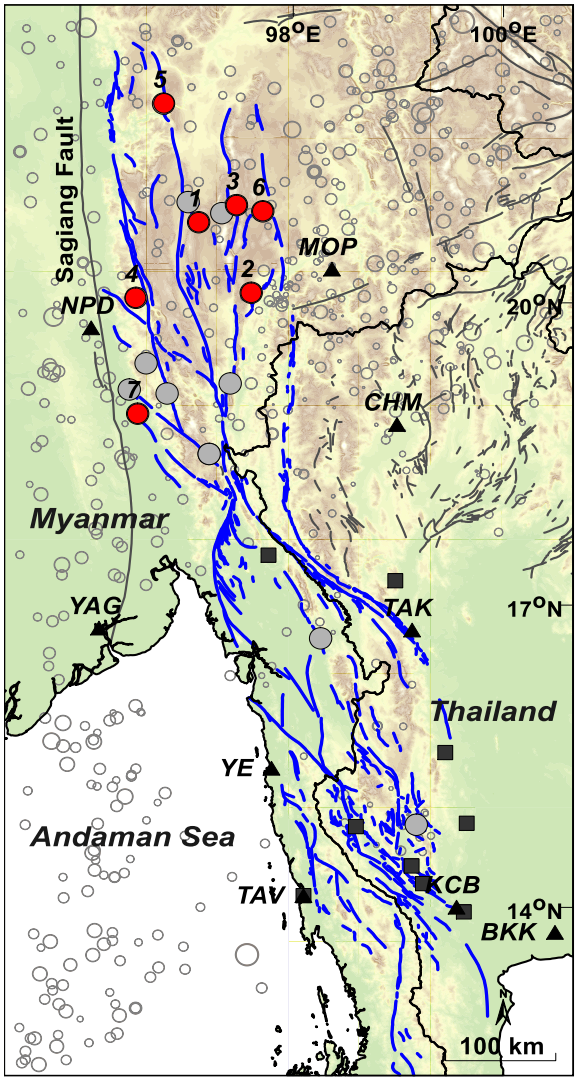

Figure 1. Map of the Thailand-Myanmar border illustrating the groups of the SSFS, as compiled by Nutalaya et al. (1985) and Pailoplee et al. (2009). White circles denote the epicentral distributions of the earthquake data after enhancement of the completeness ($M_w \geq 2.3$ recorded during 1980–2015). Grey and red circles show earthquakes with $M_w \geq 5.0$ recorded along the SSFS during 1992–2008 (see also Table 1). Triangles and squares give the locations of cities and hydropower dams, respectively.

According to Sobolev (1995), laboratory rock experiments revealed that before the rupturing process of a strong earthquake, two empirically specific stages of seismicity rates can be detected: the quiescent (seismicity decrease) and activation (seismicity increase) stages. Of these stages, seismic quiescence is an effective precursor and has been used with success in earthquake forecasting during the past four decades (e.g., Mogi, 1969; Wyss and Habermann, 1988; Wyss and Martirosyan, 1998; Wiemer and Wyss, 1994; Sukrungsri and Pailoplee, 2015). Therefore, in order to find out and constrain the prospective areas of likely upcoming earthquakes near the SSFS, as mentioned previously, the main objective of this study was to examine and detect the changes in the seismicity rate along the SSFS, from an analysis of the available seismicity data.

2. DATA AND COMPLETENESS

The significant requirement for a meaningful statistical analysis of the seismicity rate is the use of a homogeneous earthquake catalogue. In order to provide the main dataset utilized in this study, earthquake data were selected from the International Seismological Centre (www.isc.ac.uk). The scope of the area for downloading the data was extended 300 km from the study area (longitude 92.25–103.67° E and latitude 9.33–25.96° N). The depth was limited to 40 km according to the shallow crustal earthquake. As a result, 30,908 earthquake events recorded during 1964–2016 then formed the initial basis of this analysis. The recorded magnitudes of these earthquakes varied in the range of 1.0–6.5, but in different scales (M_W, m_b and M_S). Thus, to homogenize these earthquake magnitude scales, the earthquake reports in the M_S and m_b magnitude scales were converted to M_W using the empirical relationships contributed by Pailoplee (2016).

Next, to provide data that directly represented the tectonic activities, the clustered events, such as foreshocks and aftershocks, were declustered and removed according to the assumptions of Gardner and Knopoff (1974).

Empirically, inadvertent changes in the recorded magnitude shift due to changes in the recording and operating process are a common problem in earthquake catalogues and can introduce artefactual errors in seismicity rate investigations (e.g., Wyss, 1991; Zuniga and Wiemer, 1999). To detect this error, the fore-/after-shock removed earthquake catalogue was then scanned according to the GENAS procedure (Habermann, 1983) available in ZMAP (Wiemer, 2001). As a result, no serious artifact of the magnitude shift phenomena was found to exist in the earthquake data with a $M_w > 2.3$ recorded during 1980–2016, and so these 2,249 earthquakes were used as the main dataset for this analysis.

3. Retrospective Test of the Z Value

To examine the changes in the seismicity rate that were significantly related to subsequent hazardous earthquakes, the Z value statistic, as expressed mathematically in Equation (1) (Wiemer and Wyss, 1994), was employed.

$$Z = \frac{R_{bg} - R_w}{\sqrt{\frac{S_{bg}}{N_{bg}} + \frac{S_w}{N_w}}}, \quad (1)$$

where N is the number of the closest earthquake data from the investigate site (and the other terms are defined below). Thereafter, the cumulative number of all considered earthquakes was performed. In an individual time step from the starting to the end points of the recorded earthquake data, earthquakes generated within the time window (T_w) were selected and analyzed for the Z value following Equation (1). The parameters R_w and R_{bg} denote the average seismicity rate evaluated from the earthquake data inside and outside T_w. The parameters S_w and S_{bg} denote the standard deviation of R_w and R_{bg}, whereas N_w and N_{bg} are the number of earthquake events recognized inside and outside T_w, respectively. With respect to the seismicity rate, + and – of Z values imply the stages of seismic quiescence and activation, respectively, within T_w compared with the seismicity rate outside the T_w.

According to the methodology for analyzing the Z value, it is notable that the parameters N and T_w are free to vary depending on the individual site and time of interest. Therefore, in order to specify the appropriate N and T_w values in this Z value investigation along the SSFS, seven earthquakes with a $M_w \geq 5.0$ reported during 1992–2008 (Figure 1 and Table 1) were employed for retrospective testing.

Table 1. List of earthquakes with $M_w \geq 5.0$ generated along the SSFS during 1992–2008 and some results of the Z–value investigation according to the free parameter N = 25 events and T_w = 2 y. The parameter Z_{max} denotes the maximum Z value evaluated at each epicenter of the earthquake case study, while Qs and Q-time are the starting time of seismic quiescence and the time span between the mentioned quiescence stage and the earthquake case study, respectively.

No.	Longitude (ºE)	Latitude (ºN)	Date (d/m/y)	Time (UTC)	Depth (km)	M_w	Z_{max}	Qs (y)	Q-time (y)
1.	97.10	20.80	25/03/1992	22:32	33	5.4	1.5	1987.9	4.3
2.	97.60	20.10	15/04/1992	01:31	33	6.0	1.8	1988.6	3.7
3.	97.46	20.97	28/10/1992	07:02	33	5.6	2.7	1988.6	4.2
4.	96.50	20.05	10/07/2001	20:56	10	5.0	6.9	1992.8	8.7
5.	96.77	21.98	18/01/2002	21:05	33	5.4	3.8	1998.8	3.3

6.	97.71	20.91	26/12/2004	01:29	39	5.8	6.7	1992.8	12.2
7.	96.52	18.90	11/11/2008	02:19	10	5.1	6.5	2001.5	7.3

In each individual retrospective case study (Table 1), the parameter N was varied from 50–200 earthquakes with a 25-event interval, while T_w was varied from 1–15 y with a 0.5-y interval. Therefore, a total of 210 (7 x 30) paired conditions were analyzed iteratively for the seismicity rate change in each earthquake case study where both the temporal and spatial distributions of the Z value were estimated for each earthquake case study.

3.1. Temporal Investigation

In the temporal investigation, a circle was drawn around each epicenter of the earthquake case studies, and its radius was then increased until it included the N number of earthquakes. Thereafter, the cumulative number of the considered earthquake data versus time was plotted starting at 1980 and ending at the occurrence time of each earthquake case study. For each T_w moving through time at steps of 14 d, the Z value was calculated according to Equation (1). After the iterative tests for all the conditions mentioned above, it was found that using N = 25 events and T_w = 2 y gave the ability to detect the significant maximum Z value prior to the occurrence time of all seven earthquake case studies in the SSFS (Table 1). Thus, these values were defined as the most suitable ones, and the cumulative number of earthquakes and the variation of Z with time obtained when using them are illustrated in Figure 2.

For instance, in Figure 2a, an anomalous quiescence with a comparatively high maximum Z value (1.5) began at about 1987.9 and had a duration (Q-duration) of about 4.3 y before the M_w-5.4 earthquake generated at the northern Mandalay on March 25th, 1992. In Figures 2b and 2c, a decreased seismicity rate (Z = 1.8 and 2.7) was found at the same time (1988.6) followed by the M_w-6.0 and M_w-5.6 earthquakes on April 15th, 1992 and October 28th, 1992, respectively. Another obvious quiescence stage (Z = 6.9) started at 1992.8 before the M_w-5.0 earthquake on July 10th, 2001, which was 8.7 y after the quiescence was detected (Figure 2d). For the earthquake shown in Figure 2e, there was a comparatively short time span of a decreasing seismicity rate (Z = 3.8) at 1998.8, some 3.3 y before the M_w-5.4 earthquake generated on January 18th, 2002. In Figures 2f and 2g, the Z curve of the M_w-5.8 and M_w-5.1 earthquakes illustrated two-time spans of seismic quiescence with a calculated maximum Z around 6.7–6.5. However, this work defined the last peak (at 1992.8 and 2001.5, respectively), as the respective starting point of the quiescent stage (12.2–7.3 y before the occurrence of the hazardous earthquakes), because the occurrence time of the last quiescent stage developed close to the earthquake case study.

According to the temporal Z values illustrated in Figure 2, it was noticeable that there was some prominent seismic quiescence associated with the subsequent earthquake in that area. However, the time span between the quiescence period and the subsequent earthquake (Q-duration) varied from 3.3–12.2 y, and so the calculated Z value when using N = 25 events and T_w = 2 y is likely to be useful for intermediate-term (months to a decade) earthquake forecasting in the SSFS.

3.2. Spatial Investigation

To confirm the existing seismic quiescence defined in Figure 2, the Z value was also evaluated spatially and mapped. To achieve this, the area covering the SSFS (longitude 95.25–100.67^o E and latitude 12.33–22.96^o N) was gridded at an interval of 0.05^o. In each individual grid, the 25 closest earthquake data were collected, and the Z value was analyzed temporally. Based on the quiescence stage, as illustrated by the transparent strip in Figure 2, the Z values at the defined quiescence stage (Qs in Table 1) in all grid nodes were collected, contoured and then mapped (Figure 3).

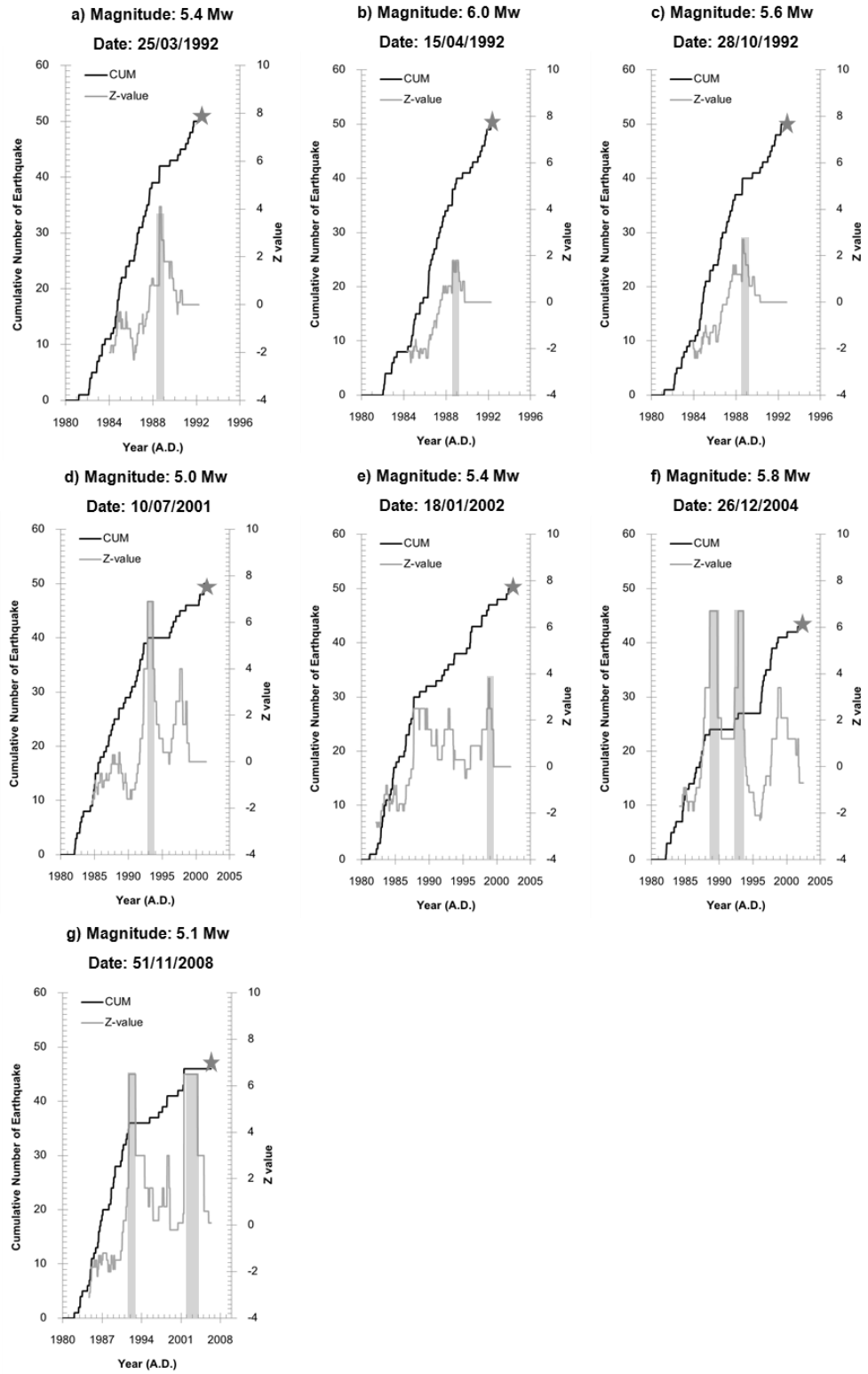

Figure 2. Temporal variation of the cumulative number of earthquakes (black line) overlaid by the Z value (grey line) evaluated at the epicenter of seven strong earthquakes (star)The Z value that was defined as the significant stage of quiescence is highlighted by a transparent strip. All Z are analyzed from the earthquake data (www.isc.ac.uk).

a) 5.4 M_w, 25/03/1992, Qs = 1987.9

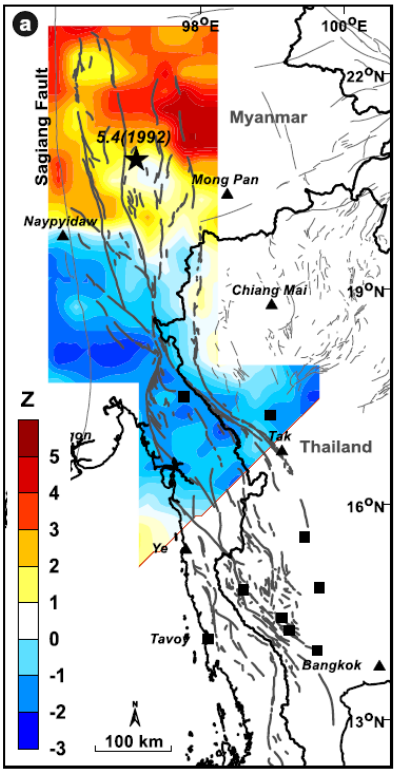

b) 6.0 M_w, 15/04/1992, Qs = 1988.6

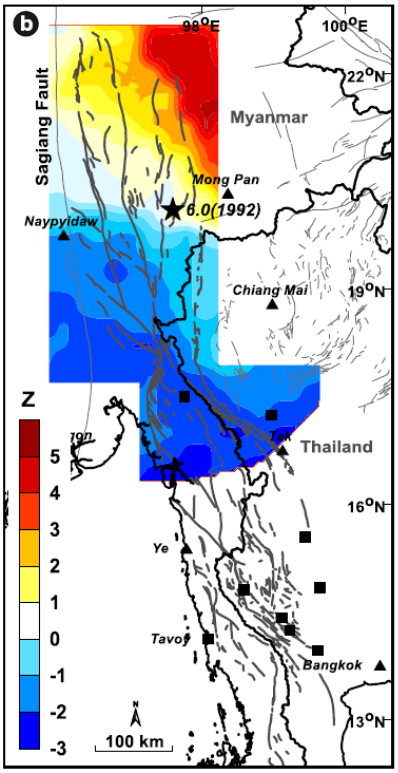

c) 5.6 M_w, 28/10/1992, Qs = 1988.6

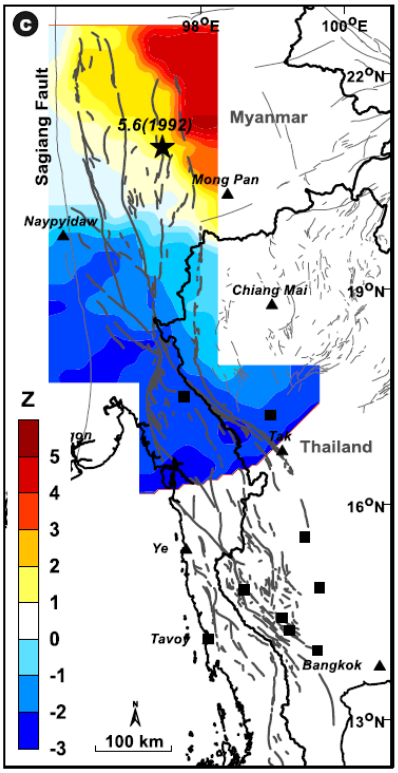

d) 5.0 M_w, 10/07/2001, Qs = 1992.8

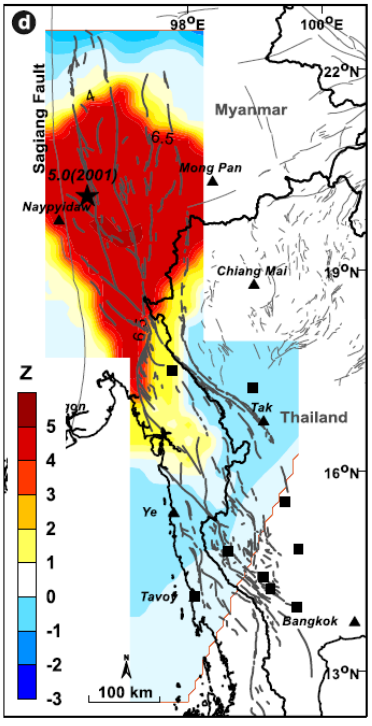

e) 5.4 M_w, 18/01/2002, Qs = 1998.8

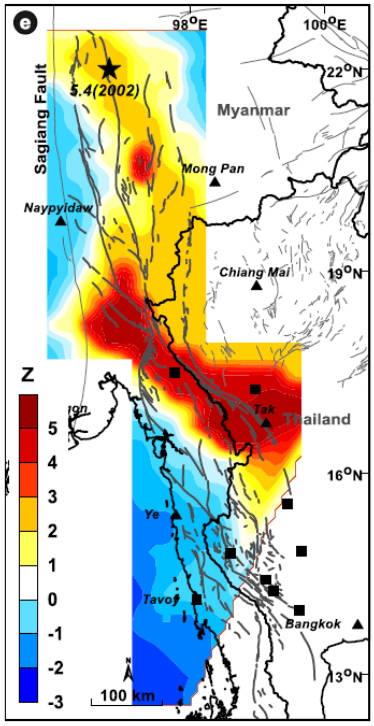

f) 5.8 M_w, 26/12/2004, Qs = 1992.8

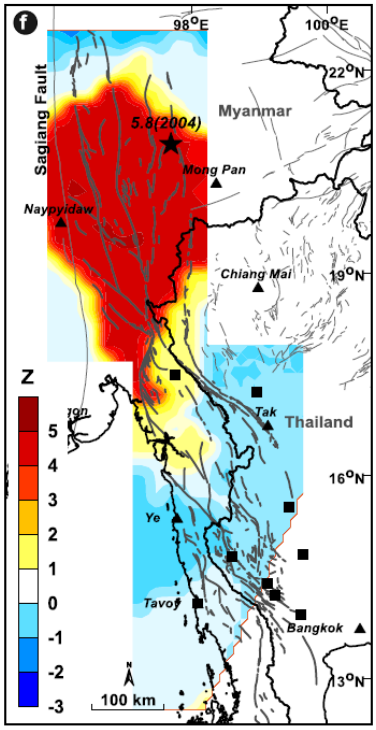

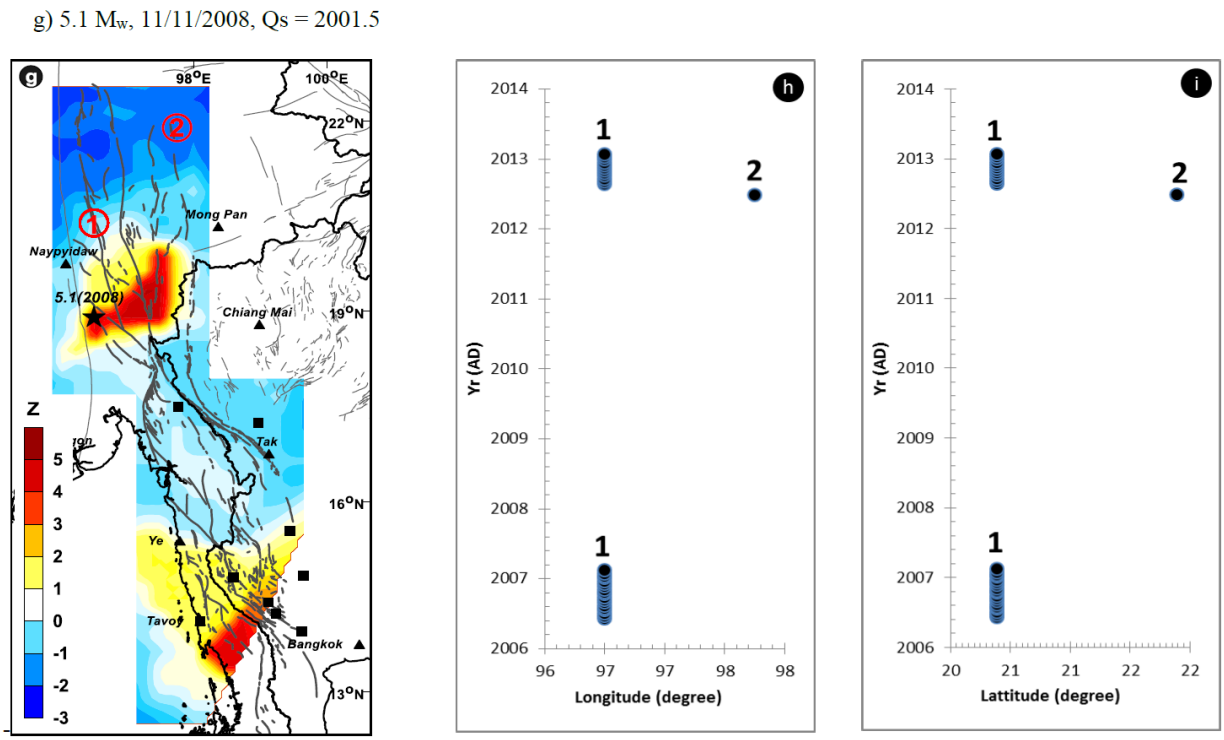

Figure 3. Map of the SSFS showing the spatial distribution of the Z values analyzed in this study (the highlighted time slice of each respective map shown in Figure 2). Red and blue colors (from a to g) represent high and low Z values, respectively, that imply the quiescence and activation stages in the seismicity rate, respectively. Black stars indicate the epicenters of major earthquakes considered in this study.

For instance, in Figure 3a (Qs = 1987.9), the spatial distribution of the Z value revealed a comparatively high Z value in the northern most part of the SSFS. Thereafter, around 4.3 y later the epicenter of the M_w-5.4 main shock posed on March 25th, 1992 was located in the southern rim of the mentioned anomaly.

During 1988.6 an anomalous Z value (1.8–2.7) was evident in the northwestern part of the SSFS at the northern part of Mong Pan (Figures 3b and 3c). Around 3.7–4.2 y later in 1992, the mainshocks of 6.0 M_w and 5.6 M_w were generated in the southern rim of this mentioned anomaly.

In addition, in 1992.8, a prominent anomalous high Z value (3.8–6.5) was evident over the northern segment of the SSFS where the M_w-5.0 (Figure 3d) and M_w-5.8 (Figure 3f) earthquakes were posed within this anomaly in 2001 and 2004, respectively.

Meanwhile, in 1998.8 (Figure 3e), Z anomalies of up to 6.7 were detected in a NW-SE direction along the central part of the SSFS, including a small pocket of anomalies located on the western part of Mong Pan. Although, the M_w-5.8 earthquake posed on December 26th, 2004 was out of the maximum Z, the location of the earthquake was still in the vicinity of the quiescent stage (i.e., positive Z value of 3.8; Figure 3g). Finally, the scoped anomaly of Z = 6.5 was evident in the southern part of Naypyidaw and was followed by the M_w-5.1 earthquake around 7.3 y later on November 11th, 2008 (Figure 3e).

Based on the good relationship between the comparatively high Z values (seismic quiescence) and the subsequent earthquake location, the use of N = 25 events and T_w = 2 y allowed the obtained high Z values to reliably indicate the precursory seismic quiescence of the forthcoming earthquakes along the SSFS.

4. PRESENT-DAY INVESTIGATION

Using the effective free parameters of N = 25 events and T_w = 2 y derived in the previous section, the Z value was then investigated according to the present-day seismicity recorded during 2005–2015 with a stepping interval of 14 d. The results revealed that the maximum Z anomalies (Z = 7.3) were defined (i) in 2006.43–2007.12 and 2012.64–2013.07 at northwestern Naypyidaw (96.50^o E, 20.39^o N) and (ii) in 2012.49 at 97.75^o E, 21.89^o N in the northeastern part of the SSFS (Figures 3h and 3i).

Compared with the FMD b-value map proposed previously by Pailoplee (2016), the high Z value anomalies at the northeastern Naypyidaw conform to the comparatively low FMD b-value. Meanwhile the anomalies in the northeastern part were shifted northwards from the anomalies previously highlighted by the FMD b-value analysis (Pailoplee, 2016). Therefore, the SSFS has a high possibility of initiating strong-to-major earthquakes soon in the vicinity of (i) northwestern Naypyidaw and the (ii) northeastern part of the SSFS.

Regarding the earthquake activities, Pailoplee (2014) analyzed the FMD coefficient (a- and b-values) and revealed that in the prospective area of northwestern Naypyidaw, the possible maximum earthquake magnitude that might be posed during the next 10–50 y is 4.8–6.2 M_w, while for the northeastern part of the SSFS it was around 5.0–6.0 M_w. The recurrence intervals of earthquakes with a magnitude of 5.0, 6.0 and 7.0 M_w were around 4, 45 and 75 y and 8, 45 and 370 y for the northwestern Naypyidaw and northeastern part of the SSFS, respectively.

5. DISCUSSION AND CONCLUSION

To obtain an effective earthquake precursor, significant changes in the seismicity rate were investigated in terms of the Z value along the SSFS. After enhancement of the available earthquake catalogue, the 2,249 earthquakes with a $M_w \geq$ 2.3 recorded during 1980–2016 were collected as the completeness portion of the seismicity data and were used in this seismicity investigation. In order to determine the appropriate free parameters N and T_w along the SSFS, seven available moderate

earthquakes (M_w > 5.0) reported since 1990 were tested iteratively with a variety of paired N and T_w values, where the use of N = 25 and T_w = 2 y clearly defined a significant high Z value (quiescence) before all of the seven subsequent earthquake case studies. For instance, temporal variations revealed a significant maximum high Z value (2.7 in 1988.6) that coincided with the occurrence of the M_w-5.6 earthquake in 1992, 4.2 y after the quiescent period (Figure 2c). In addition, in 1992.8, a prominent anomalous high Z value (3.8–6.5) was evident over the northern segment of the SSFS where the M_w-5.0 (Figure 3d) and M_w-5.8 (Figure 3f) earthquakes were subsequently posed in 2001 and 2004, respectively. This successful correlation of the precursory high Z value and the subsequent earthquake in the same area implied that the Z-value parameters of N = 25 and T_w = 2 y could be used to detect the current day precursory seismic quiescence along the SSFS.

For investigation of the present-day 2005–2015 seismicity data, the maximum Z value (7.3) was detected (i) in 2006.43–2007.12 and 2012.64–2013.07 at northwestern Naypyidaw (96.50^o E, 20.39^o N) and (ii) in 2012.49 at 97.75^o E, 21.89^o N at the northeastern part of the SSFS (Figures 3g–i). This agrees well with those areas proposed previously by the FMD b-value analysis (Pailoplee, 2016). Therefore, effective mitigation plans should be urgently contributed, in particular for Naypyidaw, the new capital city of Myanmar.

ACKNOWLEDGEMENTS

This research This research was supported by the Ratchadapiseksomphot Endowment Fund 2020 of Chulalongkorn University (CU_GR_63_158_23_24). We thank the Office of Research Affairs, Chulalongkorn University, for a critical review and improved English. We acknowledge thoughtful comments and suggestions by the editors and anonymous reviewers that enhanced the quality of this manuscript significantly.

REFFERENCES

Charusiri, P., Kosuwan, S., Saithong, P., Khaowiset, K., Pananont, P., Thitimakorn, T., and Pailoplee, S., 2011, Active fault study in Kanchanaburi province, Western Thailand. Technical report, Thailand Research Fund, Bangkok, Thailand, 252p. [in Thai with English abstract]

Department of Mineral Resources, 2007, Paleo-earthquake along the Sri Sawath and Three Pagoda Fault Zones, Kanchanaburi province. Technical report, Department of Mineral Resources, Bangkok, Thailand, 127p. [in Thai with English abstract]

Gardner, J.K., and Knopoff, L., 1974, Is the sequence of earthquakes in Southern California, with aftershocks removed, Poissonian?. Bulletin of the Seismological Society of America, 64, 363−367.

Gutenberg, B., and Richter, C.F., 1944, Frequency of earthquakes in California. Bulletin Seismological Society of America, 34, 185−188.

Habermann, R.E., 1983, Teleseismic detection in the Aleutian Island Arc. Journal of Geophysical Research, 88, 5056–5064.

Mogi, K., 1969, Some feature of recent seismic activity in and near Japan (2), Activity before and after great earthquake. Bulletin of the Earthquake Research Institute, Tokyo, 47, 395–417.

Nutalaya, P., Sodsri S., and Arnold, E.P., 1985, Series on seismology-volume II-Thailand. In E.P Arnold (ed.), Technical report, Southeast Asia Association of Seismology and Earthquake Engineering, 402p.

Nuttee, R., Charusiri, P., Takashima, I., and Kosuwan S., 2005, Pakeo-

earthquakes along the southern segment of the Sri Sawat fault, Kanchanaburi, western Thailand: Morphotectonic and TL-dating evidence. Proceedings of the International Conference on Geology, Geotechnology and Mineral Resources of Indochina (GEOINDO 2005) 28-30 November 2005, Khon Kaen, Thailand, 542–554.

Pailoplee, S., 2014, Earthquake activities along the strike-slip fault system on the Thailand-Myanmar border. Terrestrial, Atmospheric and Oceanic Sciences, 25, 483−490.

Pailoplee, S., 2016, Mapping of b-value anomalies along the strike-slip fault system on the Thailand–Myanmar border: Implications for upcoming earthquakes. Journal of Earthquake and Tsunami, 10, 1671001-1−13.

Pailoplee, S., and Charusiri, P., 2016, Seismic hazards in Thailand: a compilation and updated probabilistic analysis. Earth, Planets and Space, DOI: 10.1186/s40623-016-0465-6.

Pailoplee, S., Sugiyama, Y., and Charusiri, P., 2009, Deterministic and probabilistic seismic hazard analyses in Thailand and adjacent areas using active fault data. Earth, Planets and Space, 61, 1313–1325.

Rhodes, B.P., Perez, R., Lamjuan, A., and Kosuwan, S., 2004, Kinematics and tectonic implications of the Mae Kuang Fault, northern Thailand. Journal of Asian Earth Sciences, 24, 79−89.

Sobolev, G.A., 1995, Fundamental of Earthquake Prediction. Electromagnetic Research Centre, Moscow. 161p.

Sukrungsri, S., and Pailoplee, S., 2015, Precursory seismicity changes prior to major earthquakes along the Sumatra-Andaman subduction zone: a region-time-length algorithm approach. Earth, Planets and Space, DOI 10.1186/s40623-015-0269-0.

Wells, D.I. and Coppersmith, K.I. 1994. New empirical relationship among magnitude, rupture, width, rupture area, and surface displacement. Bulletin of the Seismological Society of America 84, 974-1002.

Wiemer, S., 2001, A software package to analyse seismicity: ZMAP. Seismological Research, 72, 373−382.

Wiemer, S., and Wyss, M., 1994, Seismic quiescence before the Landers (M = 7.5) and Big Bear (M = 6.5) 1992 Earthquakes. Bulletin of the Seismological Society of America, 84, 900–916.

Wyss, M., 1991, Reporting history of the central Aleutians seismograph network and the quiescence preceding the 1986 Andreanof Island earthquake. Bulletin of the Seismological Society of America, 81, 1231–1254.

Wyss, M., and Habermann, R.E., 1988, Precursory seismic quiescence. Pure and Applied Geophysics, 126, 319–332.

Wyss, M., and Martirosyan, A., 1998, Seismic quiescence before the M7, 1988, Spitak earthquake, Armenia. Geophysical Journal International, 134, 329–340.

Zuniga, F.R., and Wiemer, S., 1999, Seismicity patterns: are they always related to natural causes?. Pageoph, 155, 713−726.

Wintle, A.G. and Murray, A.S. 1999. Luminescence sensitivity changes in quartz. Radiation Measurements 30(1), 107-118.

Won-in, K. 1999. Neotectonic Evidence along the Three-Pagoda Fault Zone, Changwat Kanchanaburi. M. Sc. Thesis, Department of Geology,

Chulalongkorn University, Bangkok, Thailand, 214p.

Wong, I., Fenton, C., Dober, M., Zachariasen, J. and Terra, F. 2005. Seismic hazard evaluation of the Tha Sae project, Thailand. Technical report, Punya Consultants Co. Ltd., 118p.

Wood, S.H. 2001. Slip rate estimate from offset stream valley volume, and dedudation rate: Mae Chan, Northern Thailand. EOS. Trans. Am. Geophys. Union 82, pp.932.

Yunan Seismological Bureau 1997. Three Pagoda Fault Zone from downstream of KhaoLaem dam to Sai Yok waterfall. Technical report, Yunan Seismological Bureau, Yunan Province, China.

Zander, A, Duller, G.A.T. and Wintle, A.G. 2000. Multiple and single aliquot luminescence dating techniques applied to quartz extracted from Middle and Upper Weichselian loess, Zemechy, Czech Republic. Journal of Quaternary Sciences 15(1), 51-60.

Zoback, M.L. 1992. First-and second-order patterns of stress in lithosphere: The World Stress Map Project. Journal of Geophysical Research 97, 11703-11728.